Supplemental Figures and Legends

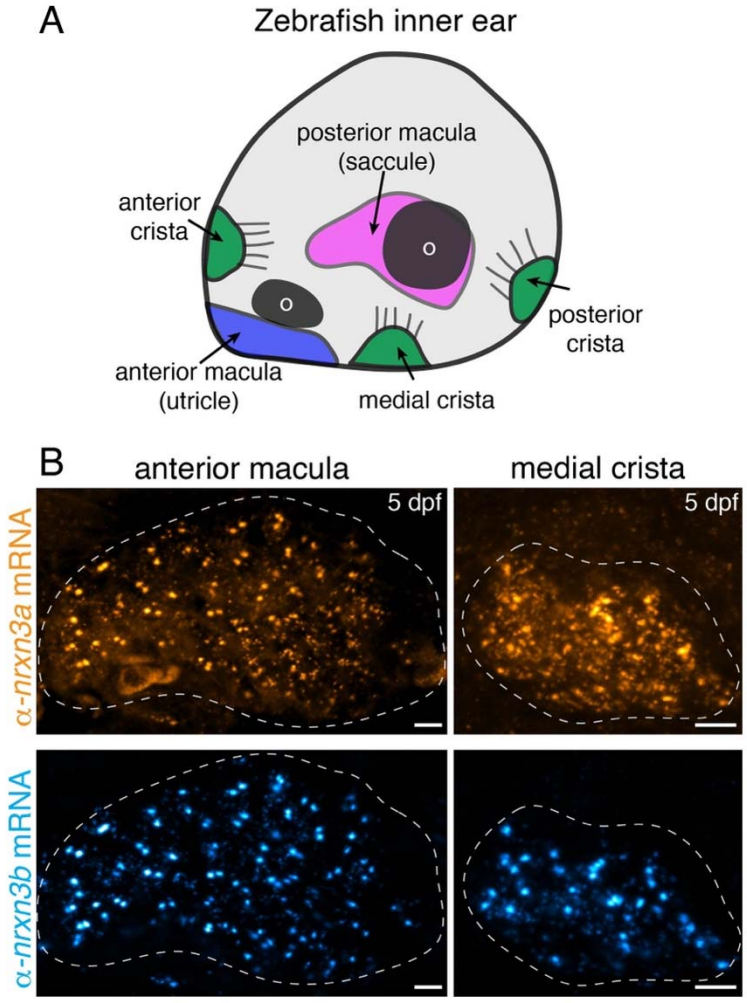

Fig S1. *nrxn3a* and *nrxn3b* mRNAs are present in zebrafish inner-ear hair cells

(**A**) Schematic showing a larval zebrafish inner ear. Within the inner ear, clusters of hair cells are present in 3 cristae and 2 maculae. Each macula is associated with an otolith (o). (**B**) RNA FISH analysis reveals that both *α-nrxn3a* (orange) and *α-nrxn3b* (cyan) mRNAs are present in inner-ear hair cells. The dashed line in B outlines the locations of hair cells within the sensory epithelium. Images are from larvae at 5 dpf. Scale bars = 5 µm in B.

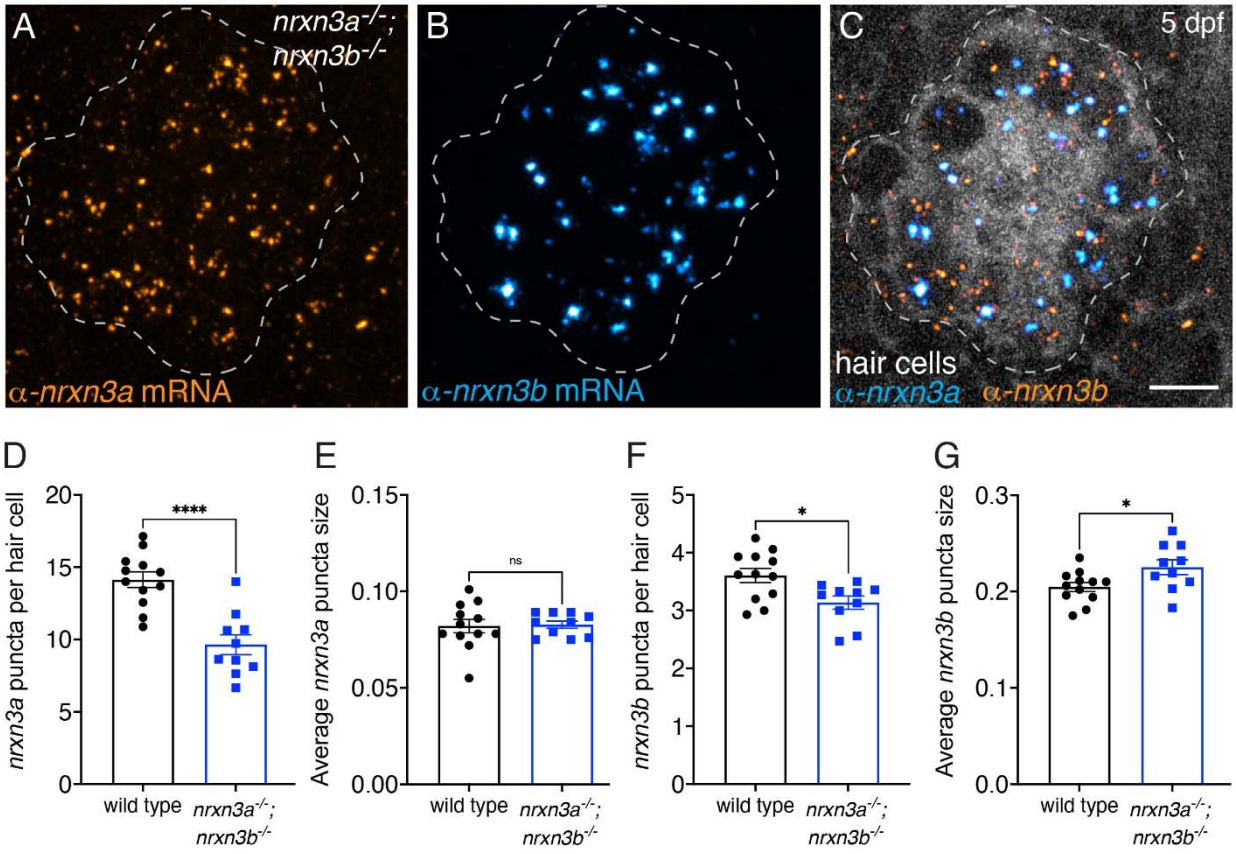

Fig S2. *nrxn3a* and *nrxn3b* mRNAs are reduced in lateral-line hair cells in zebrafish *nrxn3a; nrxn3b* mutants

(**A-C**) RNA FISH reveals that both *α-nrxn3a* (A, orange) and *α-nrxn3b* (B, cyan) mRNAs are present in lateral-line hair cells of *nrxn3a; nrxn3b* mutants. In C, hair cells (*myo6b:memGCaMP6s*) are labeled in grayscale. The dashed lines in A-C outline the locations of hair cells. (**D-G**) Quantification reveals that the number of *α-nrxn3a* (D) and *α-nrxn3b* (F) puncta are reduced in *nrxn3a; nrxn3b* mutants compared to wild-type controls. In addition, the size of *α-nrxn3b* (G), but not *α-nrxn3a* (E) puncta are slightly larger in *nrxn3a; nrxn3b* mutants compared to wild-type controls. An unpaired t-test was used in D-G, n = 12 wild-type and 10 *nrxn3a; nrxn3b* mutant neuromasts at 5 dpf. ns $P > 0.05$, *$P < 0.05$, ****$P < 0.0001$. Scale bar = 5 µm in C.

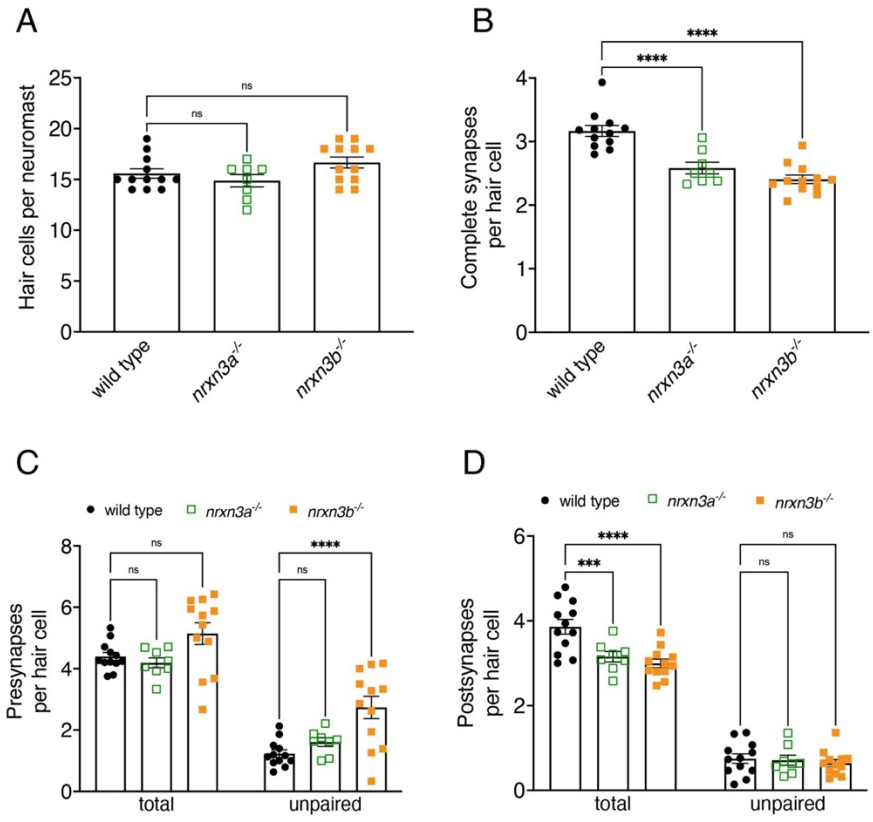

Fig S3. Minor defects in synapse organization are observed in *nrxn3a* and *nrxn3b* single mutants in mature hair cells at 5 dpf.

(**A-F**) Quantification reveals that both *nrxn3a* and *nrxn3b* single mutants have a similar number of hair cells per neuromast compared to wild-type controls (A). There are significantly fewer complete synapses per hair cell in *nrxn3b* and *nrxn3a* single mutants compared to wild-type controls (B). The total number of pre-synapses are the same across all genotypes but there are significantly more unpaired presynapses in *nrxn3b* mutants (C). The total number of postsynapses per hair cell is significantly reduced in both in *nrxn3b* and *nrxn3a* single mutants compared to wild-type controls. In contrast, the number of unpaired postsynapses per hair cell is the same across all genotypes (D). N = 12 wild-type, 8 *nrxn3a* and 12 *nrxn3b* mutant neuromasts in A-D at 5 dpf. A one-way ANOVA was used in A-B, while a 2-way ANOVA was used in C-D. ns $P > 0.05$, *$P < 0.05$, ***$P < 0.001$, ****$P < 0.0001$.

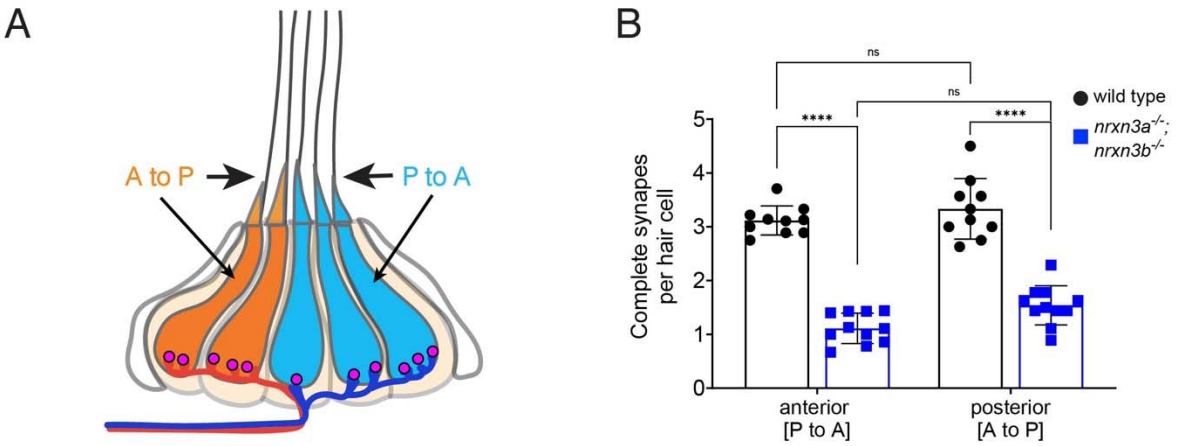

Fig S4. Synapse loss in mature hair cells is not linked to hair-cell orientation

(A-B) In primary posterior lateral-line neuromasts there are two populations of hair cells. One responds to anterior flow (blue, A), while the other responds to posterior flow (orange, A). Each population is selectively innervated by distinct afferent neurons (blue and orange processes). There is a significant and equivalent reduction in the number of complete synapses in hair cells that respond to anterior and posterior flow in *nrxn3a; nrxn3b* mutants compared to wild-type controls (B). N = 10 wild-type and 11 in *nrxn3a; nrxn3b* mutant neuromasts at 5 dpf. A 2-way ANOVA was used in B. ns $P > 0.05$, ****$P < 0.0001$.

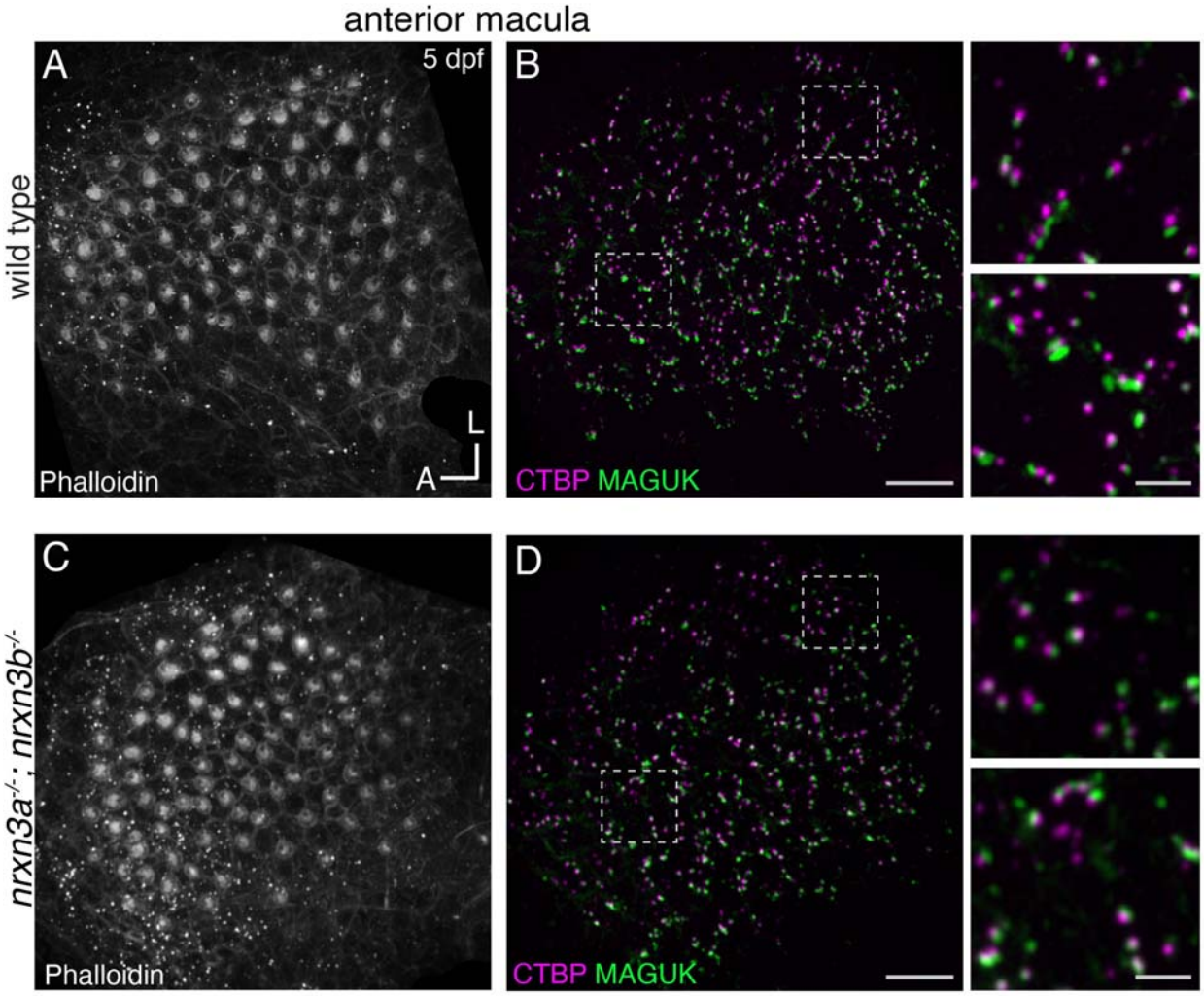

Fig S5. Loss of Nrxn3 results in fewer synapses hair cells in the zebrafish anterior macula

(**A-D**) Confocal images of the anterior macula (utricle) in wild-type controls (A-B, top panels) and *nrxn3a; nrxn3b* mutants (C-D, bottom panels). Phalloidin labels the apical hair bundles (A,C) while CTBP labels the presynapses (magenta), and MAGUK labels postsynapses (green) in B and D. The dashed lines indicate regions used to create the insets on the right side of panels B and D. The higher magnification insets show that there are fewer complete synapses in *nrxn3a; nrxn3b* mutants compared to wild-type controls. Images were taken from larvae at 5 dpf. Scale bars = 10 µm in A-D, 5 µm in the insets.

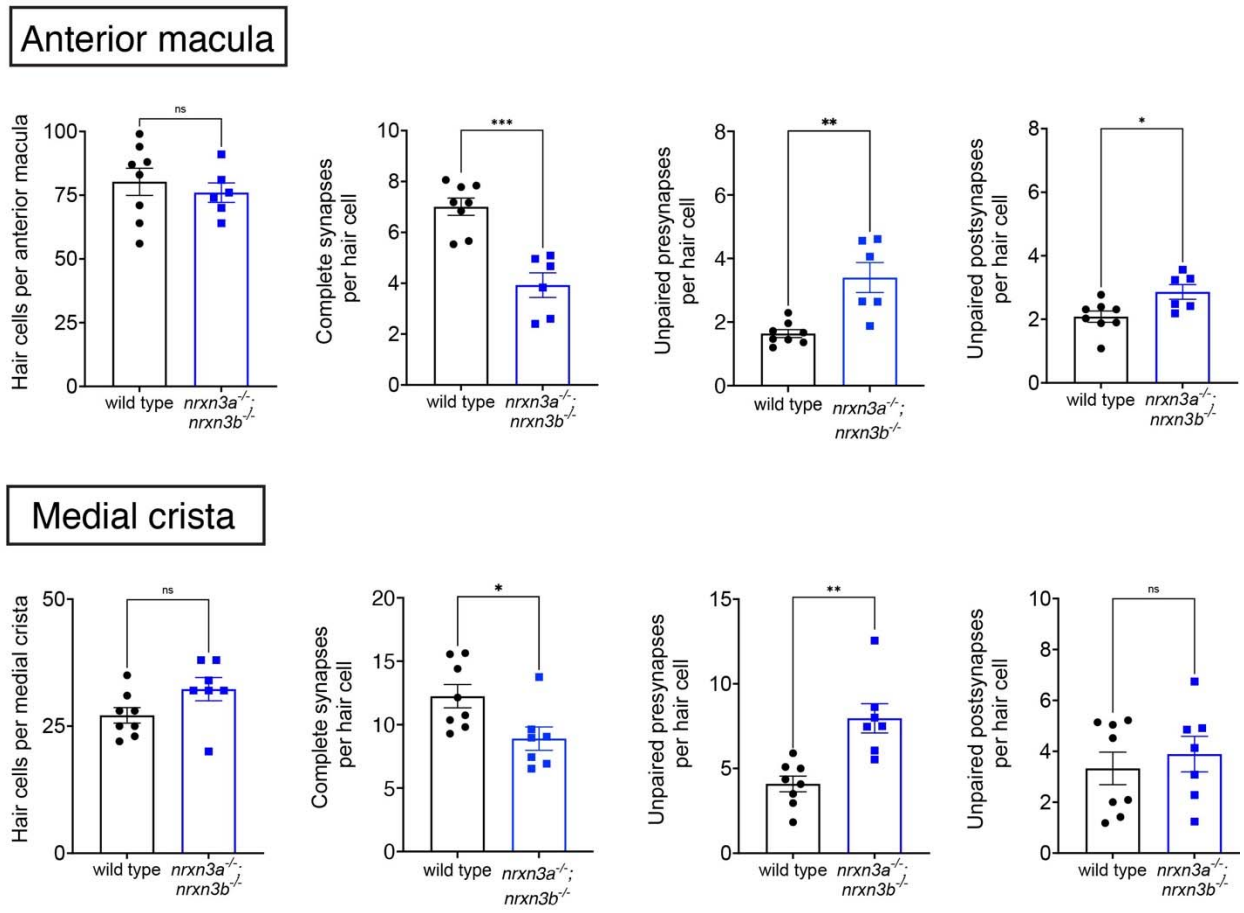

Fig S6. Quantification of synapse loss in anterior macula and medial crista in *nrxn3a; nrxn3b* mutants

Quantification reveals that wild-type controls and *nrxn3a; nrxn3b* mutants have a similar number of hair cells per anterior macula and medial crista. There are significantly fewer complete synapses per hair cell in each epithelium in *nrxn3a; nrxn3b* mutants compared to wild-type controls. Along with fewer complete synapses, there are significantly more unpaired presynapses per hair cell in *nrxn3a; nrxn3b* mutants compared to wild-type controls in both the anterior macula and medial crista. There are also more unpaired postsynapses per hair cell in the anterior macula, but not the medial crista in *nrxn3a; nrxn3b* mutants compared to wild-type controls. N = 8 wild-type and n = 6 *nrxn3a; nrxn3b* mutant anterior maculae, n = 8 wild-type and n = 7 *nrxn3a; nrxn3b* mutant medial cristae. Quantifications are from larvae at 5 dpf. An unpaired t-test was used for comparisons. ns $P > 0.05$, *$P < 0.05$, **$P < 0.01$, ***$P < 0.001$.

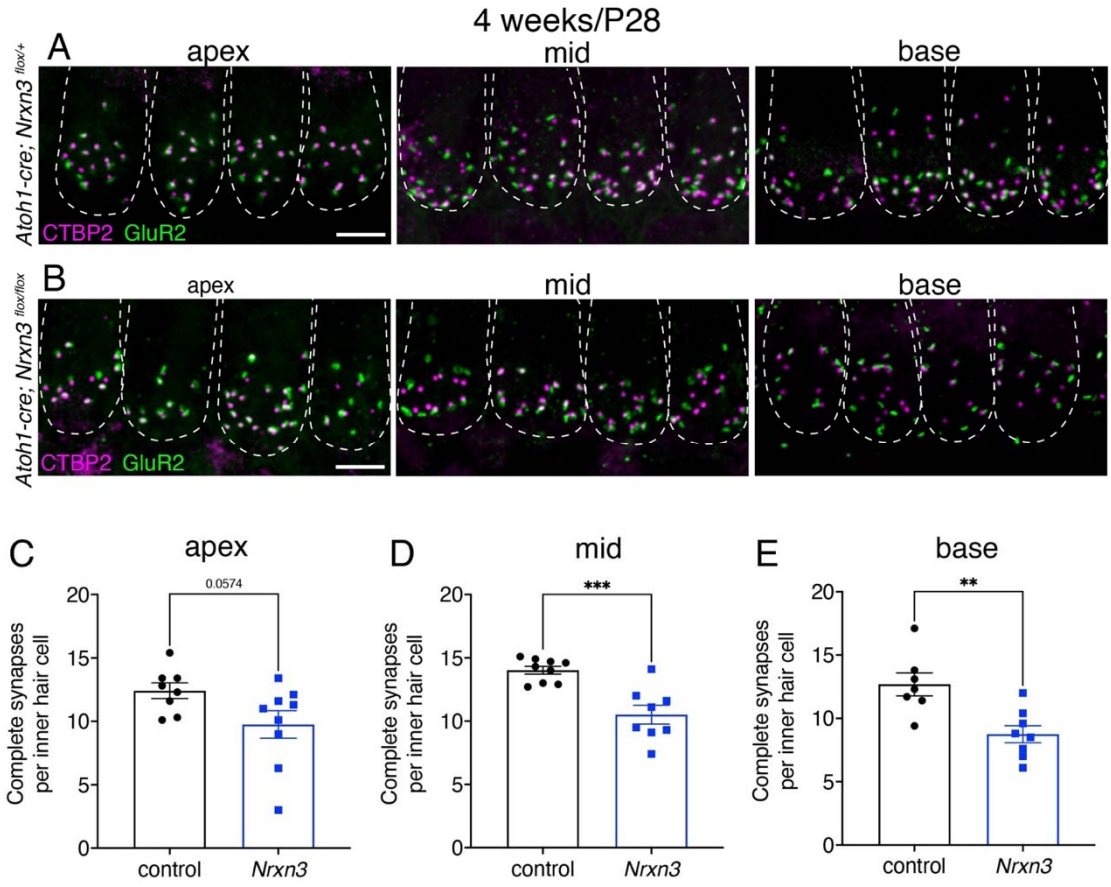

Fig S7. NRXN3 is required at 4 weeks for proper synapse numbers in mouse auditory inner hair cells

(**A-B**) Confocal images of 4-week old (P28) mouse inner hair cells from control (A) and *Nrxn3* mutant animals (*Atoh1-Cre; Nrxn3*$^{flox/flox}$) (B). CTBP2 is used to label the presynapses (magenta), and GluR2 is used to label the postsynapses (green). Merged images show 4 IHCs from 3 different regions of the cochlea (apex, middle, basal thirds) for each genotype. Dashed lines indicate the outlines of hair-cell bodies in each image. (**C-E**) Quantification reveals that compared to controls, *Nrxn3* mutants have significantly fewer complete synapses per inner hair cell at the mid (D) and base (E), and a reduced but not significant decrease at the apex (C). N = 61 control and 58 *Nrxn3* IHCs for the apex region, 65 control and 59 *Nrxn3* IHCs for the for mid region, 50 control and 60 *Nrxn3* IHCs for the for base region. These findings were compiled from 4 animals from each genotype. An unpaired t-test was used in C-E. **P < 0.01, ***P < 0.001. Scale bar = 5 µm in A.

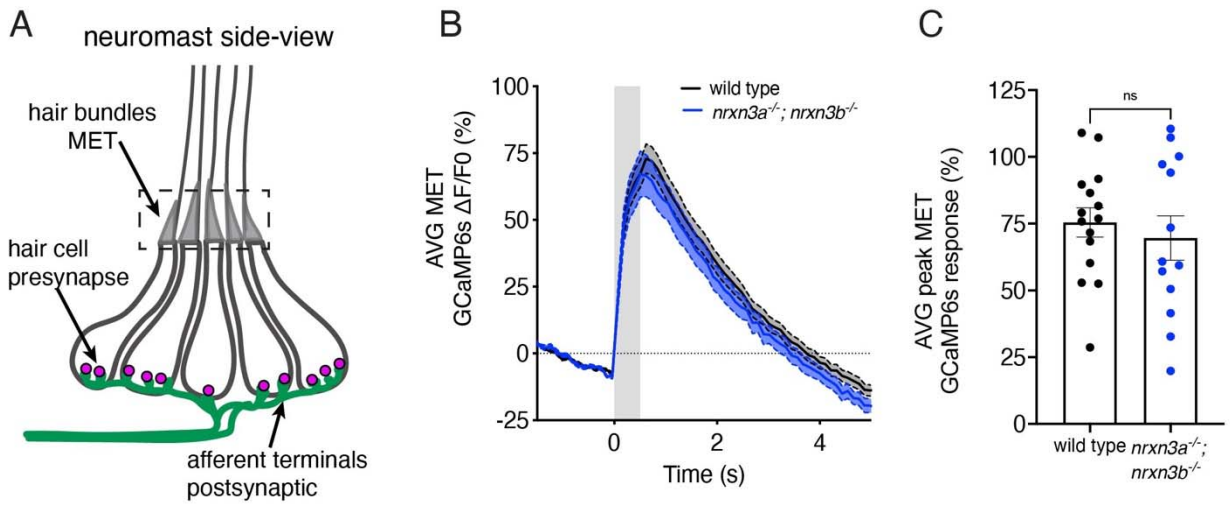

Fig S8. Loss of Nrxn3 does not impact the magnitude of mechanosensitive responses in lateral-line hair cells.

(A) Schematic of a neuromast shown from the side. The region used to measure mechanosensitive GCaMP6 responses (MET) in apical hair bundles is indicated with a dashed box. (**B**) ΔF/F0 GCaMP6s traces showing average MET GCaMP6 response during a 500 ms fluid-jet stimulation (grey area) for wild-type controls (black) and *nrxn3a; nrxn3b* mutants (blue). Traces are displayed as mean, dashed lines are SEM. (**C**) Maximum ΔF/F0 MET calcium GCaMP6 during stimulation for wild-type controls (black) and *nrxn3a; nrxn3b* mutants (blue). N = 15 wild-type and 13 *nrxn3a; nrxn3b* mutant neuromasts at 5-6 dpf. An unpaired t-test was used in C. ns $P > 0.05$.

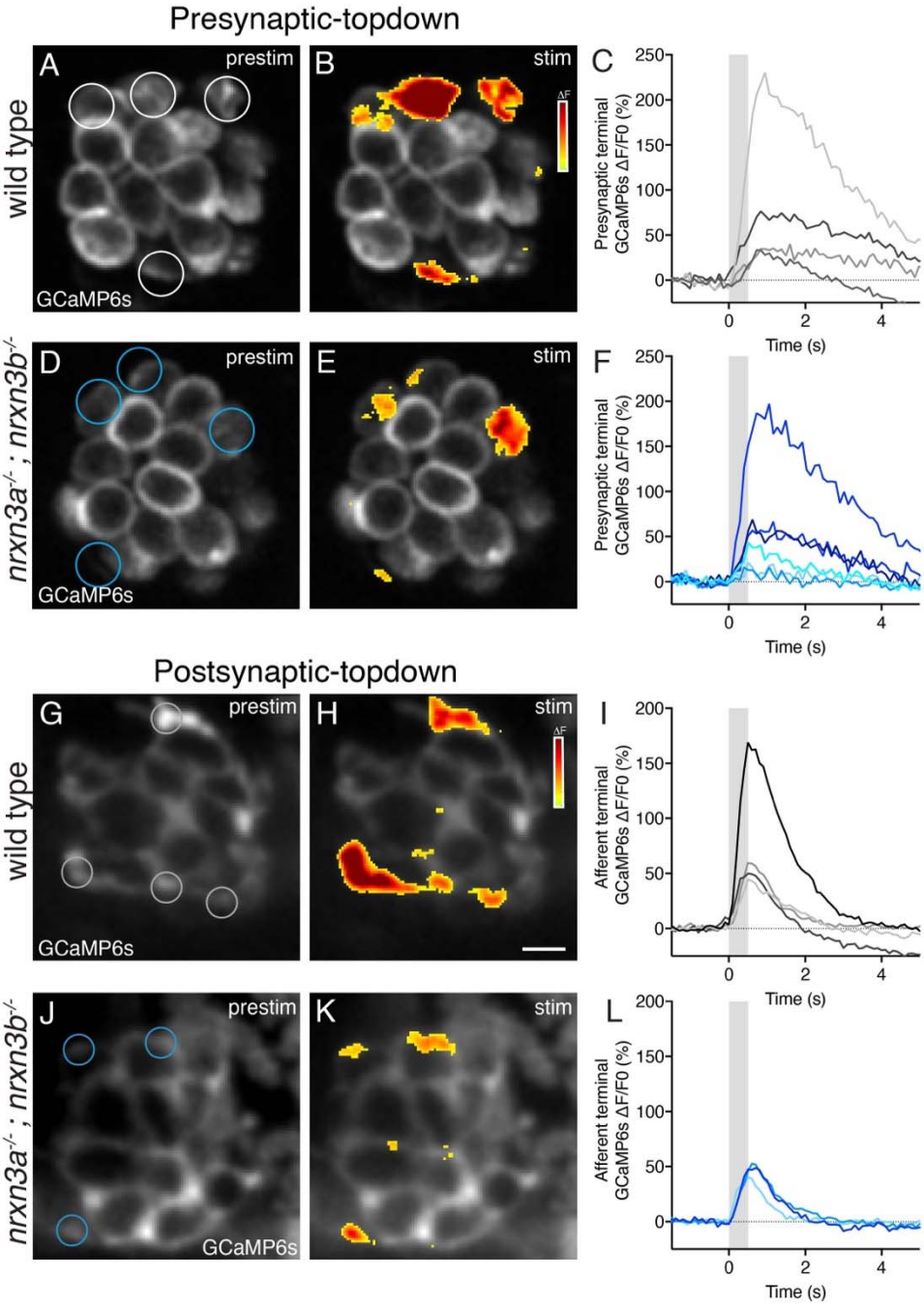

Fig S9. Nrxn3 is required for proper hair-cell synapse function in the lateral line.

(**A-F**) ΔF heatmaps show spatial patterns of presynaptic GCaMP6s increases in hair cells before (A,D) and during (B,E) a 500 ms fluid-jet stimulation in a wild-type (A,B) and *nrxn3a; nrxn3b* mutant (D,E) neuromast. ROIs indicate synaptically active hair cells and examples of regions used to measure the average response per neuromast. Traces in C and F show ΔF/F responses from ROIs in A and D. Gray area indicates timing of stimulus. (**G-L**) ΔF heatmaps show spatial

1197 patterns of postsynaptic GCaMP6s increases in hair cells before (G,J) and during (H,K) a 500 ms
1198 fluid-jet stimulation in a wild-type (G,H) and *nrxn3a; nrxn3b* mutant (J,K) neuromast. ROIs
1199 indicate synaptically active terminals and examples of regions used to measure the average
1200 terminal response per neuromast. Traces in I and J show ΔF/F responses from ROIs in G and J.
1201 Gray area indicates timing of stimulus. Wild-type examples in A-B and G-H correspond to the
1202 same example in Fig 6 C,D and G,H.
1203
1204